On the Temperature Percolation in a w/o Microemulsion in the Presence of Organic Derivatives of Chalcogens

S. K. Mehta,* Shweta Sharma, and K. K. Bhasin

Department of Chemistry and Centre of Advanced Studies in Chemistry, Panjab University, Chandigarh-160014, India

Received: January 5, 2005; In Final Form: March 18, 2005

The course of temperature percolation in a w/o microemulsion system comprising water/bis(2-ethylhexyl) sulfosuccinate sodium, AOT/isooctane affected by the presence of additives has been investigated. Additives, viz., organic derivatives of chalcogens including dipyridyl diselenide (Py_2Se_2), diphenyl diselenide (Ph_2Se_2), and dipyridyl ditelluride (Py_2Te_2), have been assimilated in the reverse micellar system. Formulations have been studied in terms of (i) the concentration variation of additives, (ii) the change in ω (= $[H_2O]/[AOT]$), and (iii) the change in the nonpolar continuum, S (= [oil]/[AOT]). Phenyl derivatives hinder the percolation, whereas the pyridyl derivative in moderate amounts favors the phenomenon. The estimated values of the critical exponents are lower than those predicted by the dynamic percolation theory. The association model has been implemented to access the thermodynamic parameters of droplet clustering. Pyridyl compounds are expected to alter the rigidity of the surfactant monolayer, which could help to promote the attractive interdroplet interaction. FT-IR spectroscopy has been used to elucidate the changes occurring in the core water in the presence of organic derivatives of chalcogens as the droplet size is increased. Results have been rationalized in terms of the alteration in the physicochemical behavior of the water/AOT/isooctane microemulsion in the presence of additives.

Introduction

Microemulsions are thermodynamically stable, isotropic dispersions of oil and water stabilized by the solubilization property of surfactants. They have often been described as spherical droplets of the dispersed phase separated from the continuous phase by a film of surfactant.[1−3] The aggregates formed in the reverse micellar system possess three solubilization sites: the apolar continuum, the micellar interface, and the intramicellar water pool. Thus, microemulsion can provide a simultaneous environment for both hydrophilic as well as lyophillic compounds in accordance with their physicochemical nature.[4−6]

Recent years have witnessed an increasing interest in assimilating various additives to the microemulsion system.[7−15] It has been shown by Meier[16] that the assimilation of poly(ethylene oxide) to the water/AOT/isooctane micellar system affects the elastic bending modulus, K, and modifies the membrane curvature. The effect of additives (viz., alkanols, crown ethers, and esters) on the water/AOT/decane microemulsion has been investigated by Mukhopadhay et al.,[17] where additives offer flexibility to the surfactant interface. Very recently, Garcia-Rio et al.[18] have analyzed the effect of crown ethers to complexate and solubilize Na^+ in the interface of the AOT/isooctane/water microemulsion. The effect of NaCl on the phase behavior and percolation threshold of water/SDS + Myrj45/cyclohexane in the presence of various alcohols has been reported by Dogra and Rakshit.[19]

Of the different physical properties of the w/o microemulsion, the intriguing phenomenon of conductance percolation is striking, where a manifold (100−1000 times) increase in the conductance takes place when either the temperature, θ, or the volume fraction, ϕ (system composition), approaches the critical value (i.e., θ_c or ϕ_c, respectively). The occurrence of percolation reveals that cluster size, attractive interactions, and the rate of exchange of material between the droplets through collision increase. Water droplets come in close contact during percolation, and two major effects—channel formation and the blockening effects—govern the role that the additives play in altering the threshold level. It has been proposed[20] that the onset of percolation occurs in the microemulsion when interdroplet interactions exceed the critical value of $2kT$. Although this area has been quantified with adequate theories,[21−24] the network of the percolation mechanism is fragmented.

We undertook a comprehensive experimental study of temperature-induced percolation in an AOT-based w/o microemulsion affected by the presence of some organic derivatives of chalcogens (oxygen family). The influence of these organochalcogens, including dipyridyl diselenide (Py_2Se_2), diphenyl diselenide (Ph_2Se_2), and diphenyl ditelluride (Ph_2Te_2), has been examined at constant microemulsion composition. These diphenyl and dipyridyl selenides/tellurides contain bulky selenium and tellurium bridged between the phenyl or pyridyl groups (Scheme 1).

The conductivity−temperature data has been treated to estimate the activation energy of clustering, ΔE_p, and the energetics of percolation, which includes the derivation of free energy (ΔG^o_{cl}), enthalpy (ΔH^o_{cl}), and entropy (ΔS^o_{cl}) values associated with the clustering. The droplet association has been worked out on the basis of the pseudophase model of micellar aggregate formation. The epilogue of the article consists of the effects of additive concentration, droplet size (ω = $[H_2O]/[AOT]$), and nonpolar continuum concentration (S = [oil]/[AOT]). The hydration of the surfactant with solubilized water

* Corresponding author. E-mail: skmehta@pu.ac.in. Tel: +91-172-2534423. Fax: +91-172-2545074.

10.1021/jp050052g CCC: $30.25
Published on Web 04/19/2005

SCHEME 1: Molecular Structure of Organic Derivatives of Chalcogens

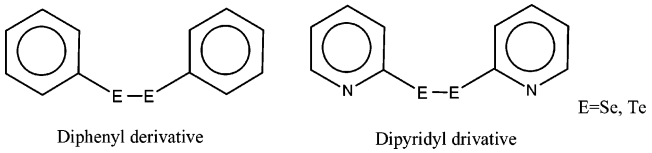

and the consecutive effect of the additives have been investigated by means of FT-IR analysis. The stabilized colloids have been studied in light of any physical or chemical transformation going on within the microemulsion droplets. A comparison of the pronounced effect of organic derivatives of chalcogens has been made by considering the systems without any additive.

Materials and Methods

Materials. Microemulsions were prepared by mixing appropriate amounts of surfactant, oil, and water. Bis(2-ethylhexyl) sulfosuccinate sodium salt, AOT (Fluka, purity >99%), and isoocatne (E-Merck, purity >99%) were used as received. Organochalcogens including Ph_2Se_2, Py_2Se_2, and Ph_2Te_2 as crystalline solids were synthesized in the laboratory and characterized through spectroscopic techniques.[25−27] The water used for the microemulsion preparation was triply distilled with a conductivity value $<0.3\ \mu S\ cm^{-1}$.

Methods. *(i) Conductance Measurements.* The conductivity of microemulsion systems was measured in a thermostatic glass cell with the help of a PICO digital conductivity meter operating at 50 Hz from Labindia Instruments. Electrodes were inserted in a double-walled glass cell containing the microemulsion. The cell constant of the cell used was 1.00 cm^{-1}, and conductivity measurements were carried out with an absolute accuracy of up to ±3%. The temperature of the sample was maintained by an RE320 Ecoline thermostat controlled to better that ±0.01 K temperature variation. Sufficient time was given for equilibration between successive measurements.

(ii) Spectroscopic Measurements. FT-IR spectra were recorded in the frequency range of 4400−350 cm^{-1} with the help of a Perkin-Elmer (RX1) FT-IR spectrometer using AgCl plates.

(iii) Microemulsion System. In the AOT microemulsion, prepared above the critical micellar concentration ($\sim 10^{-3}-10^{-4}$ mol dm^{-3}), the droplets are fairly monodisperse spherical water pockets coated with a monomolecular layer of surfactant molecules.[22] The size of the droplets is essentially determined by the water to surfactant molar ratio, ω (= $[H_2O]/[AOT]$), and the concentration of the oil phase is given by S (= [oil]/[AOT]). For the system with variation in S (= 5−15), ω has been kept constant at 22.0, whereas for the systems studied with variation in ω (= 15−40) S is fixed at 9.7. The temperature range for the conductivity measurements is taken between 284.15 and 343.15 K.

Results and Discussion

Conductivity Measurement. Electrical conductivity measurements have been used to assess the microemulsion formation and probe the structural changes occurring in the system.[8−11,16−19]

(i) Percolation Course and Effect of the Additives. The percolation threshold has been investigated in the microemulsion systems with increasing concentrations of different organochalcogens. Figure 1 shows the conductance variation with temperature in the absence and presence of Py_2Se_2, Ph_2Se_2, and Py at $\omega = 22.5$ and [AOT] = 0.415 M. Sigmoidal behavior of log σ has been observed with increasing temperature. For

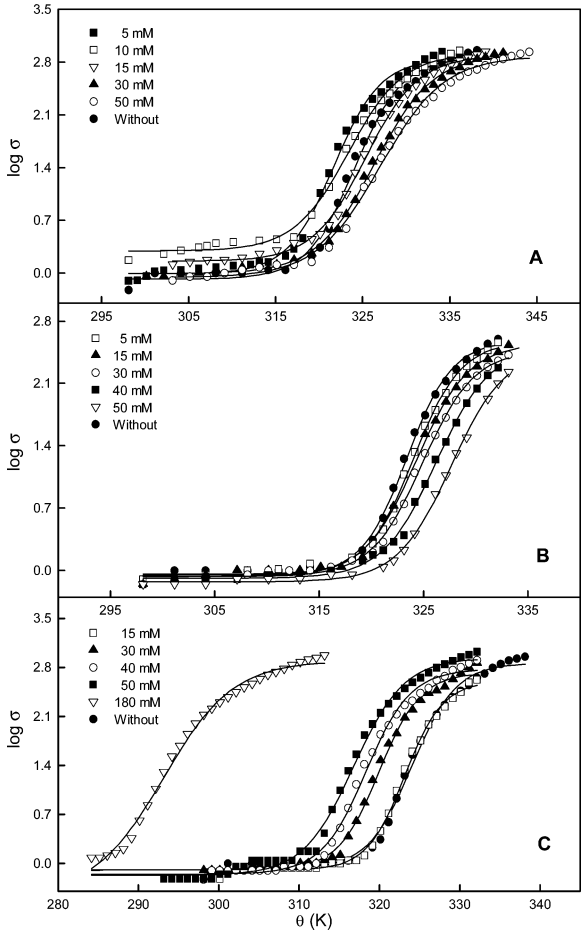

Figure 1. Variation of specific conductance with temperature at varied concentrations of different additives at $\omega = 22.5$ and [AOT] = 0.415 M. (A) Py_2Se_2; (B) Ph_2Se_2; (C) Py. (Solid lines show SBE fitting.)

constant composition, the system remains unchanged until the determinant temperature, θ_c, is reached. Fluctuations in the ion content of microemulsion droplets result in the charged droplets. An increase in temperature increases the frequency of these fluctuations, and thus an increase in conductivity is observed.[28] Both the charge-hopping and coalescence phenomena can sufficiently explain the influence of temperature on conductivity. A varied effect of organochalcogens in terms of percolation assisting or resisting entities can be visualized from Figure 1. The conductivity of the systems decreases with the addition of pyridyl and phenyl derivatives of Se except for 5 and 10 mM concentrations of Py_2Se_2. Py, however, increases the system conductance. The threshold percolation temperature is determined from the d log $\sigma/d\theta$ versus θ plot,[29] where the maxima correspond to the threshold temperature, θ_c. (Figure 2 shows the representative differential plot for obtaining θ_c for a microemulsion with Ph_2Se_2 = 10 mM at $\omega = 22$ for different values of S.) Percolation temperatures for the studied systems have been listed in Table 1.

Recently, Moulik et al.[8,29] proposed the sigmoidal Boltzman equation (SBE) to determine the threshold characteristics of microemulsion systems. In conductance percolation, the equivalent equation can be written as

$$\log \sigma = \log \sigma_f \left[1 + \left(\frac{\log \sigma_i - \log \sigma_f}{\log \sigma_f}\right)\left\{\frac{1 + \exp(\theta - \theta_c)}{\Delta\theta}\right\}^{-1}\right] \quad (1)$$

TABLE 1: Percolation Parameters and Activation Energy for the Water/AOT/Isooctane Microemulsion in the Presence of Organochalcogens at $\omega = 22.5$ and [AOT] = 0.415 M

additive	[additive] (mM)	log σ_i	log σ_f	θ_c(K) differential	θ_c(K) SBE	ΔE_p (kJ mol^{-1})	S_k
without		-0.05 ± 0.01	2.58 ± 0.04	322.22	322.54 ± 0.14	499 ± 2	
	5	-0.10 ± 0.01	2.60 ± 0.04	322.09	322.15 ± 0.12	441 ± 2	
	30	-0.10 ± 0.01	2.72 ± 0.03	319.80	319.96 ± 0.14	430 ± 2	
Py	40	-0.15 ± 0.02	2.78 ± 0.04	317.08	317.32 ± 0.16	399 ± 2	-0.17
	50	-0.17 ± 0.02	2.93 ± 0.04	314.10	314.77 ± 0.18	377 ± 3	± 0.01
	180	-0.44 ± 0.04	2.89 ± 0.04	293.05	293.15 ± 1.42	297 ± 2	
	5	-0.01 ± 0.00	2.84 ± 0.04	320.16	321.69 ± 0.16	444 ± 2	
	10	-0.29 ± 0.02	2.91 ± 0.04	322.27	322.37 ± 0.19	389 ± 1	
Py_2Se_2	15	-0.16 ± 0.02	2.88 ± 0.03	324.01	325.30 ± 0.13	377 ± 2	0.09
	30	-0.01 ± 0.00	2.90 ± 0.02	325.05	326.36 ± 0.11	357 ± 2	± 0.02
	50	-0.06 ± 0.01	2.88 ± 0.03	329.17	327.00 ± 0.16	347 ± 2	
	5	-0.04 ± 0.01	2.57 ± 0.04	323.04	323.10 ± 0.13	532 ± 2	
	15	-0.07 ± 0.02	2.55 ± 0.04	324.02	324.33 ± 0.15	447 ± 2	
Ph_2Se_2	30	-0.07 ± 0.01	2.47 ± 0.04	325.13	324.90 ± 0.13	443 ± 2	0.10
	40	-0.09 ± 0.02	2.51 ± 0.07	326.05	326.19 ± 0.19	439 ± 1	± 0.01
	50	-0.13 ± 0.01	2.48 ± 0.06	328.04	327.87 ± 0.16	423 ± 1	
Ph_2Te_2	30	-0.07 ± 0.02	2.57 ± 0.03	326.19	326.21 ± 0.16		

where i, f, and c indicate the initial, final, and percolative stages, respectively, and $\Delta\theta$ is the interval of the temperature measurement. Fitted curves of the conductance−temperature profile to the SBE are shown in Figure 1 as solid lines. The initial and final values of conductance along with the transition temperature, θ_c, obtained from the SBE fitting are given in Table 1. Good agreement can be seen in the θ_c values calculated from two different methods. The effect of additives on θ_c for the studied water/AOT/isooctane microemulsion can be visualized in three different ways: (i) With increasing concentration, θ_c increases in the presence of Ph_2Se_2 for the constant-composition microemulsion. (ii) Py_2Se_2 at 5 mM favors percolation; higher concentration, however, delays it. (iii) Py effectively favors percolation even at very high concentration (180 mM). The pronounced effect of additives on θ_c can be clearly seen by considering an equal concentration. Figure 3 shows an extensive comparison of all of the additives at 30 mM. The value of θ_c varies in the order Py < without additive < $Py_2Se_2 \leq Ph_2Se_2 < Ph_2Te_2$.

A comparison of Py- and Py_2Se_2-based systems with the microemulsion without any additive reveals that although Py favors percolation Py_2Se_2 delays the process. Maitra et al.[30] showed that in the percolative microemulsion the droplets retain their closed structure although infinite clusters are formed because of interdroplet interactions. It is only in the bicontinuous microemulsion that the solubilizate (NaCl here) comes out and aids in conduction through continuous media.

The mutual contact and bridging between droplets is due to the presence of additives either at the interface (e.g., hydrotopes and bile salts)[9] or in the core of the droplets (e.g., poly(ethylene glycol)s).[16] In case of Py, the active N-end anchors the droplet surface, whereas the aromatic ring offers local hydrophobicity. This results in the straight bridging of the nanodroplets, and conduit formation is favored. Py_2Se_2 is a rigid nonplaner moiety in which one (Py−Se−)− unit is bent, leaving the central horizontal plane (Scheme 2). It contains an electronically active −(−Se−Se−)− along with the N-end. The molecule adheres to the droplet interface, but the configuration results in staggered bridging. The phenyl derivatives of selenium and tellurium have no such active sites except for −(−Se−Se−)− and −(−Te−Te−)−, respectively, and remain in the dispersion medium, resisting droplet fusion by enhancing the blocking effect. Compared to the Se compound, the Te compound has been found to be more inert and susceptible to fast breakdown. This is due to the fact that Te is comparatively bulky and the bond length is longer in Te compounds (Table 2).[31]

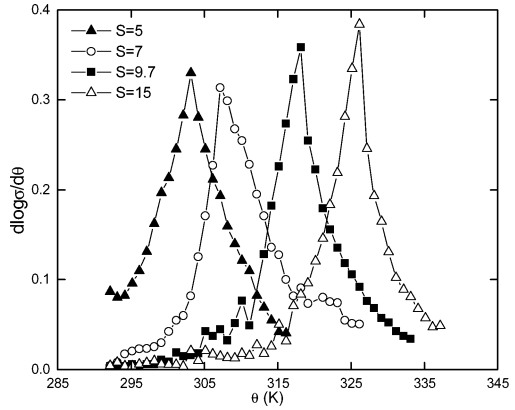

Figure 2. Variation of d log σ/dθ with temperature to observe the percolation temperature, θ_c, for [Ph_2Se_2] = 10 mM at $\omega = 22$ and $S = 5-15$ (representative plot).

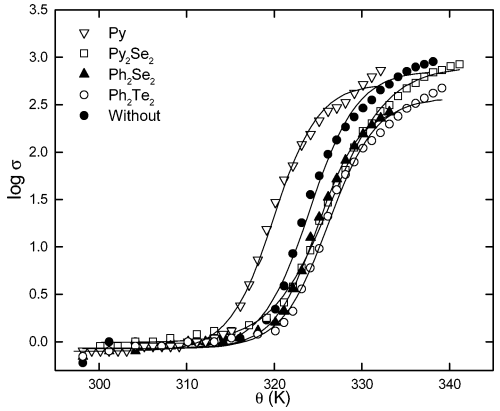

Figure 3. Variation of specific conductance with temperature for 30 mM additives at $\omega = 22.5$ and [AOT] = 0.415 M to compare the respective effect on θ_c. (Solid lines show the SBE fitting).

TABLE 2: Comparative Bond Lengths[31] of Se and Te Compounds

	bond length (Å)
C−Se	1.93−1.97
C−Te	2.1
Se−Se	≤2.3
Te−Te	≥2.7

SCHEME 2: (a) Bent Structure of Py_2Se_2[a] and (b) Fusing Droplets in the Presence of Organochalcogens

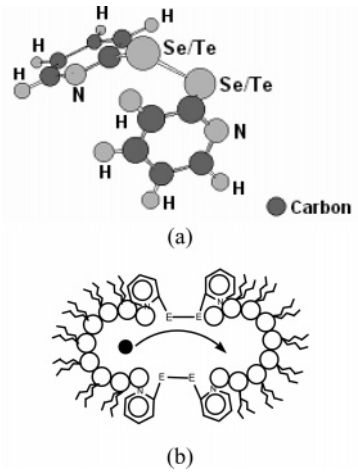

[a] In the phenyl ring, the −N− is replaced with −C−.

Moulik et al.[8] proposed the linear fit equation to estimate the efficacy of the additives in the process of percolation

$$\theta_c^a = \theta_c^o \pm S_k C \tag{2}$$

where θ_c^o and θ_c^a are the percolation temperatures without and with additive, respectively. S_k is the slope of the linear plot indicating the efficiency of additives as percolation-assisting or -resisting entities, and C is the experimental concentration of the additives. Figure 4 illustrates the linear dependence of the relation for different additives at $\omega = 22.5$ and [AOT] = 0.415 M. The slope values are presented in Table 1. S_k has been found to be negative for Py and positive for Py_2Se_2 and Ph_2Se_2. Species yielding negative slopes are percolation assistants, and solutes yielding positive slopes are percolation retardants. In terms of S_k, the efficiency order is Py > Py_2Se_2 ≥ Ph_2Se_2.

(ii) Effect of Droplet Size on the Conductivity of the w/o Microemulsion. The size of droplets in a single-phase water-in-oil or oil-in-water microemulsion is given by a geometric

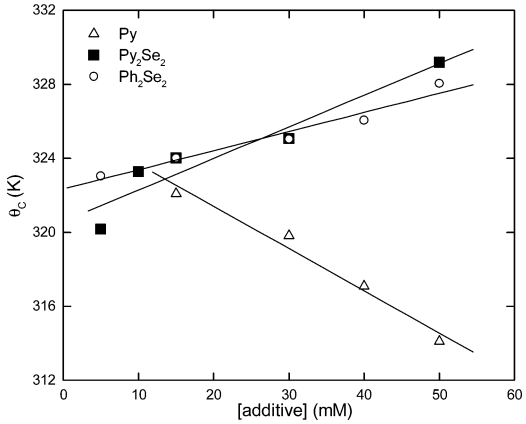

Figure 4. Percolation temperature as a function of additive concentration; the slope yields the efficacy of the additive.

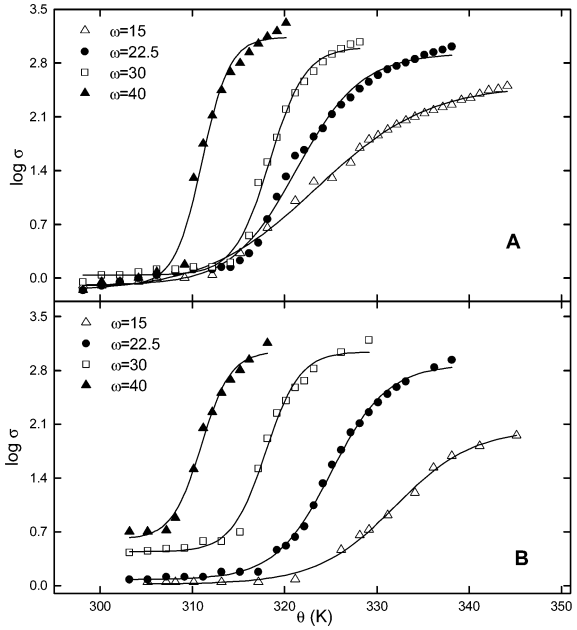

Figure 5. Variation of specific conductance with temperature for Py_2Se_2 at varied ω (= 15-40). (A) Py_2Se_2 = 5 mM; (B) Py_2Se_2 = 15 mM. (Solid lines show the SBE fitting.)

consideration (i.e., by the water to surfactant molar ratio). The effect of droplet size on the conductivity of the studied w/o microemulsion is shown in Figure 5 with sigmoidal Boltzman fitting curves for 5 and 15 mM concentrations of Py_2Se_2. The values of log σ_i, log σ_f, and θ_c along with other parameters are presented in Table 3. Figure 5 depicts that microemulsion systems at higher ω are more conducting. A decrease in θ_c has been obtained with an increase in ω for constant compositions of both formulations. An increase in droplet size is the manifestation of an increase in ω. An increase in droplet radii would increase the overlap volume between the consecutive droplets; consequently, the interaction potential increases, thereby facilitating the percolation.[32]

Eicke and Zulauf[33] observed that at $\omega > 10$ water constitute a pseudophase and a well-defined monolayer of surfactant separates the core water within the micelle. The surface free energy determines the stability of the mutually coexisting phases. The 15 mM concentration of Py_2Se_2 delays percolation to 7 K at $\omega = 15$, and the effect is reduced to ≤1 K at higher ω (30 and 40). At higher ω, the total water content of the system is increased, and the ratio of the volume of surfactant to the volume of water in the aggregates is markedly reduced, resulting in less rigidly bound structured water. Hou et al.,[34] using light scattering, found that with increasing ω the interdroplet interaction increases significantly. With increasing temperature, one can expect a decrease in the bending elasticity of the surfactant monolayer, and the additive concentration plays virtually no efficient role at higher ω.[35]

(iii) Effect of the Dispersion Medium on the Percolation Course. The effect of the solvent on the droplet interaction in the studied water/AOT/isooctane microemulsion has been visualized in light of the increase in the oil to surfactant molar ratio, S (= [oil]/[AOT]). Figure 6 depicts the temperature-induced percolation in the absence and in the presence of 10 mM Ph_2Se_2 at four different S values. The phenomenon has also been investigated for 30 mM Ph_2Se_2 at $\omega = 22.0$ and S = 9.7. The SBE fitting is shown by the solid lines in the plots, and the obtained parameters are presented in Table 3. An overall decrease in the conductance with an increase in the S value can

TABLE 3: Percolation Parameters and Activation Energy for the Water/AOT/Isooctane Microemulsion in the Absence and Presence of Organochalcogens at Varying ω (= 15−40) and S (= 5−15)

A. Water/AOT/Isooctane, $\omega = 15-40$, $S = 9.7$, and $[Py_2Se_2] = 5$, 15 mM

$[Py_2Se_2]$	$\omega =$ $[H_2O]/[AOT]$	log σ_i	log σ_f	θ_c (K) differential	θ_c (K) SBE	ΔE_p (kJ mol^{-1})
	15	-0.17 ± 0.03	2.52 ± 0.04	323.12	323.46 ± 0.30	198 ± 1
	22.5	-0.09 ± 0.02	2.93 ± 0.04	320.16	320.31 ± 0.21	444 ± 1
5 mM	30	-0.04 ± 0.01	3.01 ± 0.04	317.03	317.18 ± 0.14	573 ± 2
	40	-0.09 ± 0.03	3.14 ± 0.04	310.00	310.04 ± 0.22	867 ± 2
	15	-0.02 ± 0.01	2.04 ± 0.03	331.57	331.93 ± 0.34	184 ± 1
	22.5	-0.08 ± 0.02	2.87 ± 0.03	324.02	325.06 ± 0.14	377 ± 2
15 mM	30	-0.44 ± 0.03	3.05 ± 0.03	317.90	317.95 ± 0.21	548 ± 2
	40	-0.60 ± 0.03	3.05 ± 0.04	311.10	310.97 ± 0.22	556 ± 2

B. Water/AOT/Isooctane, $S = 5-15$, $\omega = 22.0$, and $[Ph_2Se_2] = 10$, 30 mM

[additive]	$S =$ [oil]/[AOT]	log σ_i	log σ_f	θ_c (K) differential	θ_c (K) SBE	ΔE_p (kJ mol^{-1})
	5	-0.58 ± 0.02	3.22 ± 0.05	311.10	311.53 ± 0.16	448 ± 1
without additive	7	-0.63 ± 0.01	3.03 ± 0.03	316.07	315.87 ± 0.11	489 ± 1
	9.7	-0.59 ± 0.01	2.83 ± 0.03	322.10	322.35 ± 0.12	380 ± 1
	15	-0.54 ± 0.01	2.07 ± 0.09	329.07	329.27 ± 0.40	351 ± 2
	5	-0.69 ± 0.02	3.23 ± 0.02	302.17	302.69 ± 0.06	439 ± 1
10 mM	7	-0.73 ± 0.03	2.99 ± 0.04	308.91	309.04 ± 0.17	410 ± 2
	9.7	-0.62 ± 0.01	3.00 ± 0.02	317.50	317.63 ± 0.08	401 ± 2
	15	-0.58 ± 0.01	2.87 ± 0.04	324.67	324.79 ± 0.13	466 ± 2
30 mM	9.7	-0.61 ± 0.01	2.99 ± 0.03	320.15	320.27 ± 0.11	453 ± 2

clearly be seen from the plots. The effect of the dispersion medium can be elaborated by involving the work done by Shah and Hou.[36] It has been shown that the interactions between the droplets largely determine the solubilization capacity of the formulations as the molar volume of oil is increased to a limit. The fusion of droplet pairs of constant size in temperature percolation depends on their mutual contact, which is caused by the thermal energy manifested as θ_c. (Figure 2 shows the differential plot of d log σ/dθ vs θ, that is used to locate θ_c.)

An increase in S means that the inert domain of formulation is increasing, consequently reducing the effective overlap by the moving apart of droplets. The channel formation and the resultant hopping of conducting ions is not effective, and a delay in percolation is observed. However, an interesting point has been observed on addition of Ph_2Se_2. For respective S, the value of θ_c decreases on addition of 10 mM additive at $\omega = 22.0$. The effect of the droplet surface fluidity in terms of ω and the role played by the equilibrated temperature-moderated dispersed phase may be the deciding conditions for such behavior. On addition of 30 mM Ph_2Se_2 at $S = 9.7$, the increase in θ_c compared to that for the 10 mM concentration is observed. It may be inferred that the moderate concentration of additive supported by specified formulation conditions can act as a percolation enhancing moiety.

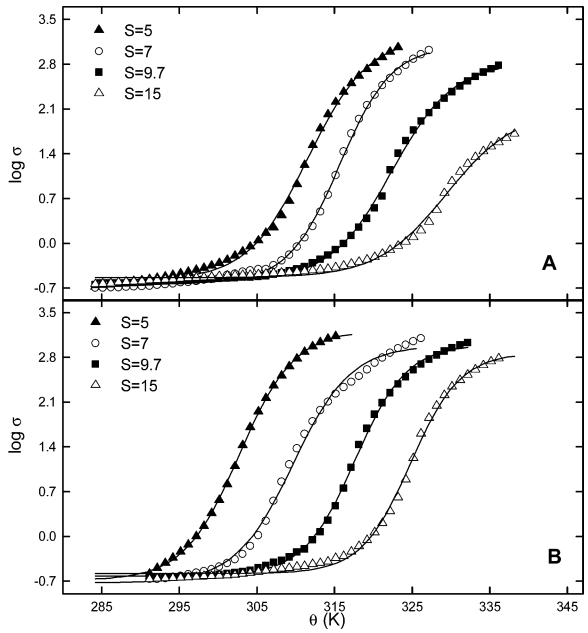

Figure 6. Conductance−temperature profile in the absence and presence of Ph_2Se_2 at $\omega = 22$ and varied S (= 15-40). (A) Without additive; (B) $Ph_2Se_2$10 mM. (Solid lines show the SBE fitting.)

(iv) Percolation and the Scaling Laws. A dramatic increase in conductivity with the droplet volume fraction of the w/o microemulsion in terms of the percolation model was given by Lagues.[37] The span of temperature percolation is also governed by two separate asymptotic power laws

$$\sigma = A(\theta_c - \theta)^{-s} \text{ where } \theta < \theta_c \text{ (below percolation)} \quad (3)$$

$$\sigma = B(\theta_c - \theta)^{t} \text{ where } \theta_c < \theta \text{ (above percolation)} \quad (4)$$

where A and B are the free parameters and s and t are the critical exponents, respectively. These laws are valid near the percolation threshold, θ_c. Figure 7 shows the log σ versus log($\theta_c - \theta$) plot for $\theta_c > \theta$ and the log σ versus log($\theta_c - \theta$) for $\theta > \theta_c$ plot, with the slopes yielding the s and t parameters, respectively. Computed values of critical exponents have been reported in Table 4. It is impossible to implicate these laws at extremely small or at limit values and in the immediate vicinity of θ_c.

From a theoretical point of view, two approaches have been proposed for the mechanism leading to percolation: one in which the static percolation model attributes the phenomenon to the appearance of bicontinuous oil and water structure and the other in which the dynamic percolation model considers the attractive interactions among water droplets and the formation of clusters due to Brownian motion. The difference between the static and dynamic percolation is reflected in terms of the deviation in the value of exponent s and t from the predicted

TABLE 4: Critical Exponents for the Water/AOT/Isooctane Microemulsion without and with Organochalcoges for (i) Additive Concentration, (ii) ω (= 15−40) Variation for Ph_2Se_2, and (iii) Variation in the *S* Value (= 5−15) for Py_2Se_2[a]

	critical exponents							
[additive]	*s*	*t*	*s*	*t*	*s*	*t*	*s*	*t*
	Py_2Se_2		Ph_2Se_2		Py			
5 mM	0.56 ± 0.05	1.43 ± 0.03	0.61 ± 0.06	1.37 ± 0.05				
10 mM	0.61 ± 0.06	1.35 ± 0.04						
15 mM	0.62 ± 0.02	1.30±0.05	0.74 ± 0.07	1.33 ± 0.01	0.82 ± 0.09	1.37 ± 0.07		
30 mM	0.77 ± 0.04	1.37±0.04	0.99 ± 0.06	1.11 ± 0.04	0.90 ± 0.09	1.29 ± 0.05		
40 mM			1.02 ± 0.08	1.15 ± 0.07	1.06 ± 0.07	1.38 ± 0.05		
50 mM	1.54 ± 0.09	0.94 ± 0.02	1.52 ± 0.04	1.03 ± 0.06	0.58 ± 0.03	1.73 ± 0.04		
180 mM					1.10 ± 0.07	1.26 ± 0.04		
	$\omega = [H_2O]/[AOT]$							
Py_2Se_2	15		22.5		30		40	
5 mM	1.09 ± 0.08	1.34 ± 0.03	0.56 ± 0.05	1.43 ± 0.04	0.40 ± 0.02	1.65 ± 0.04	0.30 ± 0.01	1.67 ± 0.02
15 mM	0.97 ± 0.08	1.01 ± 0.06	0.62 ± 0.02	1.30 ± 0.05	0.36 ± 0.03	1.05 ± 0.05	0.56 ± 0.09	1.10 ± 0.05
	$S = [oil]/[AOT]$							
Ph_2Se_2	5		7		9.7		15	
Without	1.25 ± 0.01	1.50 ± 0.02	1.24 ± 0.04	1.49 ± 0.02	1.22 ± 0.02	1.55 ± 0.04	0.84 ± 0.01	0.92 ± 0.03
10 mM	1.58 ± 0.03	1.84 ± 0.03	1.27 ± 0.06	1.73 ± 0.06	1.01 ± 0.01	1.80 ± 0.02	1.21 ± 0.04	1.24 ± 0.01
30 mM					0.91 ± 0.01	1.86 ± 0.03		

[a] Without additive at $\omega = 22.5$ and [AOT] = 0.415 M: $s = 0.64 \pm 0.05$ and $t = 1.53 \pm 0.03$.

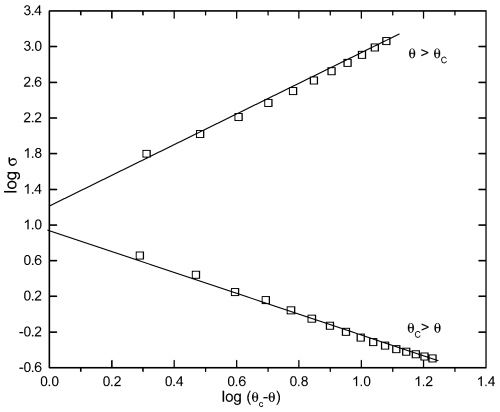

Figure 7. Variation of log σ with log($\theta_c - \theta$) without any additive at $\omega = 22$ and $S = 9.7$. The slopes yield the values of critical exponents *s* and *t*, respectively [Eqs (3) and (4)].

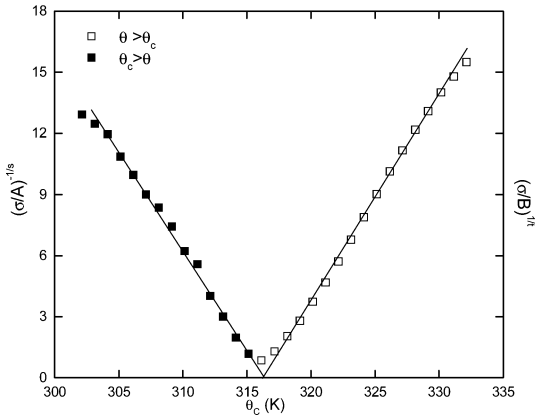

Figure 8. Variation of $(\sigma/A)^{-1/s}$ and $(\sigma/B)^{1/t}$ with temperature *t* for [Py_2Se_2] = 10 mM at $\omega = 22$ and $S = 9.7$. Deviation from the ideal value is obtained near the percolation threshold.

values. According to static theory,[38−40] the values of the critical exponents in the region above and below percolation should be $t = 1.6$ and $s = 0.7$. However, the dynamic nature makes the the exponents higher than those predicted for the static case.[41−44] For different sets of systems (i.e., with concentration variation of additives, with ω variation for Py_2Se_2, and with *S* variation for Ph_2Se_2), the value of exponent *s* lies between 0.56−1.54, 0.30−1.09, and 0.91−1.58, respectively, which are lower than the reported range (0.7−1.6).

The value of *t* falls in the ranges of 0.94−1.73, 1.05−1.67, and 0.92−1.86 for the studied systems, which are also lower compared to the literature range (1.2−2.1). Experimental data of critical exponents obtained by locating the percolation threshold as a function of temperature or volume fraction for the AOT/water/oil microemulsion with different types of oil (cyclohexane, dodecane, undecane, isooctane, etc.) had values $1.1 \le s \le 1.6$ and $1.6 \le t \le 2.2$.[45−48] In the present set of systems, the values of both the *s* and *t* parameters are lower than the ideal predicted ranges. Moulik et al.[8] put forth the analysis that the observed exponents' values are lower for percolation-resisting additives and higher for percolation-assisting additives. The additives influence the dynamics of the process and hence affect the value of both the free parameters and the critical exponents. Figure 8 depicts $(\sigma/A)^{-1/s}$ and $(\sigma/B)^{-1/t}$ plotted against θ, where good agreement can be seen between the experimental and calculated values. The resulting θ_c obtained through these plot has been observed to be closer to that obtained by the differential as well as the SBE fitting method. Good agreement has been obtained between experimental and theoretically calculated values of log σ as shown in Figure 9.

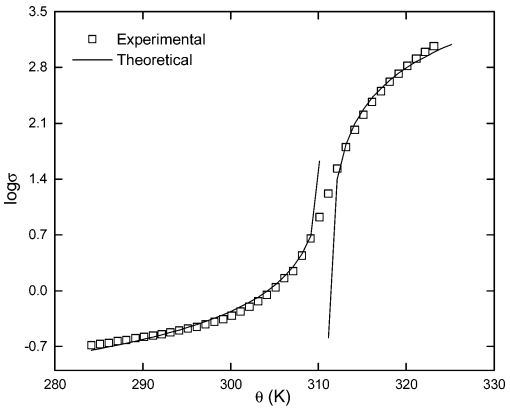

Figure 9. Representative log σ vs θ plot showing good agreement between the experimental and theoretical conductance for a microemulsion without any additive at $\omega = 22$ and $S = 5$.

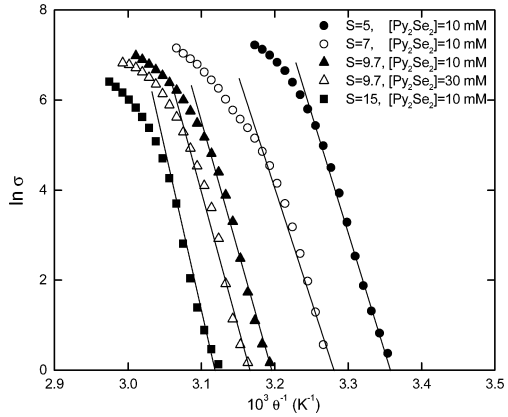

Figure 10. Arrhenius plot of ln σ vs θ^{-1} to evaluate ΔE_p for [Py_2Se_2] at $\omega = 22$ and $S = 5-15$.

(v) Activation Energy of Droplet Clustering. The activation energy of percolation in the post-percolation region has been estimated from the Arrhenius form of the relation[35,49,50]where

$$\sigma = A e^{-\Delta E_p/R\theta} \tag{5}$$

A is a constant and R and θ have their usual significance. ΔE_p has been evaluated from the slope of the linear portion of the plot of ln σ versus θ^{-1} (shown in Figure 10 for the Ph_2Se_2 = 10 and 30 mM, $\omega = 22$, and $S = 5-15$ microemulsion system). The ΔE_p values for the respective systems are given in Tables 1 and 3. For effective fusion, a pair of droplets approaching each other require a high activation energy. Fusion accelerators by way of efficient overlap help in the exchange of droplet contents, energetically favoring the process. In general, ΔE_p depends on two different contributions: the electrostatic interactions among the charged droplets and an attractive interaction resulting in the interdigitation of the surfactant tail and the solvent molecule. Quite high ΔE_p values have been obtained for the studied set of systems. Mukhopadhyay et al.[17] estimated ΔE_p for the AOT/decane microemulsion system to be 700 kJ mol^{-1} (in the absence of any additive), and the value was lowered to 300 kJ mol^{-1} in the presence of additives. Lowering of the activation energy supports easier charge transport through the oil matrix. After attaining the threshold, polar additives provide a polar microenvironment in the oil matri, and charge transport becomes convenient. The less polar or the nonpolar additives work in the reverse manner, and thus either less reduction or an increase in the ΔE_p value can be obtained, pertaining to the formation of an energy barrier. A higher value (on the order of hundreds) advocates a significant barrier, and a hopping mode of conduction is not convincing. It has been observed that the diffusion of the surfactant counterion (Na^+) through the hydrophobic region in the vicinity of two nonfusing droplets requires energy on the order of 120−150 kJ mol^{-1} or more, depending upon the conditions to which the system is subjected.[11] Bulkier Py_2Se_2, Ph_2Se_2, and Ph_2Te_2 molecules redisperse around the droplets associated with the transport of the Na^+ ion. The activated state of mass transfer thus yields a higher ΔE_p. The value of ΔE_p follows an intriguing correlation with θ_c for the respective set of systems. The phenomenon of percolation is essentially different from the normal mode of conduction, and the magnitude of ΔE_p largely depends on the separability of the droplets.

(vi) Thermodynamics of Droplet Clustering, Association Model. It is generally accepted that the threshold of electric percolation corresponds to the formation of the first open structure of an infinite cluster followed by a network of droplets.[32] The microemulsion droplets above the percolation threshold are a different phase from that of the nonpercolating droplets, with distinct physical properties. This is comparable to the pseudophase micellar model where these entities mimic the surfactant micelles. The phenomenon of clustering based upon the pseudophase model (also called the association model) can be related to the reversible fluctuation of sterically stabilized colloid particle,[51,52] and the cluster ⇄ decluster equilibrium is expected.

TABLE 5: Gibb's Standard Free Energy of Droplet Clustering, ΔG^o_{cl}, for the Water/AOT/Isooctane Microemulsion with Variation in the Concentration of Additive at $\omega = 22$ and [AOT] = 0.415 M and with Variation in ω for Py_2Se_2 (= 5, 15 mM) at $S = 9.7$

	$-\Delta G^o_{cl}$ (kJ mol^{-1})			
[additive]	Py_2Se_2	Ph_2Se_2	Py	Ph_2Te_2
5 mM	22.66	22.86		
10 mM	22.80			
15 mM	22.93	22.93	22.79	
30 mM	23.00	23.00	22.63	23.09
40 mM		23.07	22.44	
50 mM	23.30	23.21	22.22	
180 mM			20.73	
	$\omega = [H_2O]/[AOT]$			
Py_2Se_2	15	22.5	30	40
5 mM	20.84	22.54	23.78	24.50
15 mM	21.38	22.81	23.84	24.59

ΔG^o_{cl} (in the absence of any additive) = −22.80 kJ mol^{-1}

The dilution of percolating microemulsion lowers the conductivity rapidly until the clusters dissociate to the individual droplet below θ_c: the phenomenon corresponds to the process of demicellization when the surfactant concentration is lowered below the critical micellization concentration (cmc). This concept has been invoked upon by the Moulik group[8−10,53] and Alexandridis et al.[32] to estimate the thermodynamics of the clustering of droplets. The standard free energy for the transfer of 1 mol of droplet from an infinitely dilute solution to the percolating cluster, ΔG^o_{cl}, is calculated from

$$\Delta G^o_{cl} = R\theta \ln X_d \tag{6}$$

where X_d is the mole fraction of the droplets corresponding to the percolation threshold. Estimated ΔG^o_{cl} has been reported in Table 5 for variation in the concentration of additives and variation in the water to surfactant molar ratio, ω. Application of the Gibbs−Helmholtz equation allows us to calculate the standard enthalpy of cluster formation, ΔH^o_{cl}, as

$$\Delta H^o_{cl} = \frac{\partial(\Delta G^o_{cl}/\theta_c)}{\partial(1/\theta_c)} \tag{7}$$

Finally, the standard entropy of cluster formation per mole of droplet, ΔS^o_{cl}, is given by the relation

$$\Delta S^o_{cl} = \frac{\Delta H^o_{cl} - \Delta G^o_{cl}}{\theta_c} \tag{8}$$

To estimate ΔH^o_{cl}, ΔG^o_{cl} is plotted as a function of inverse percolation temperature (Figure 11), the slope yielding the value of ΔH^o_{cl}. Computed thermodynamic parameters for the microemulsion system with variation in composition (i.e., the S value) are listed in Table 6. ΔG^o_{cl} has been obtained as negative for all of the formulations, indicating the spontaneous formation of

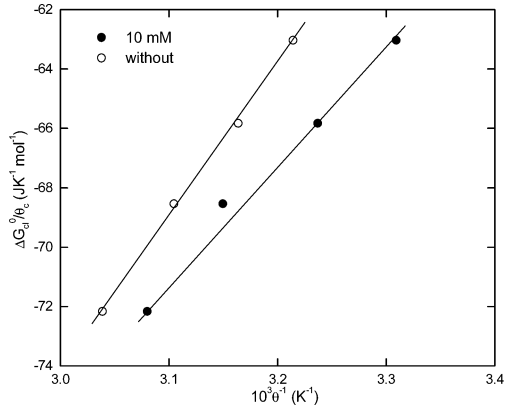

Figure 11. $\Delta G_{cl}^{o}/\theta_c$ as a function of θ^{-1} to evaluate ΔH_{cl}^{o} of clustering in the absence and presence of $[Ph_2Se_2] = 10$ mM at $\omega = 22$.

TABLE 6: Energetic Parameters of Droplet Clustering for the Water/AOT/Isooctane Microemulsion without and with Ph_2Se_2 (= 10 mM) at $\omega = 22$ for Varying [AOT] and *S*

$[Ph_2Se_2]$	S = [oil]/[AOT]	$-\Delta G_{cl}^{o}$ (kJ mol^{-1})	ΔH_{cl}^{o} (kJ mol^{-1})	ΔS_{cl}^{o} (J K^{-1} mol^{-1})
	5	19.61		
without	7	20.81	51 ± 1	228
	9.7	22.07		
	15	23.75		
	5	19.05		
10 mM	7	20.34	39 ± 2	191
	9.7	21.76		
	15	23.43		

the droplet cluster. ΔH_{cl}^{o} and ΔS_{cl}^{o} obtained for the microemulsion system without and with Ph_2Se_2 (= 10 mM) are positive (i.e., an enthalpically disfavored endothermic process). The clustering phenomenon is essentially accompanied by (i) the removal of oil barriers surrounding the dispersed droplets and (ii) the association of droplets. The first step is endothermic, whereas the second is associated with the release of heat and thus is exothermic.[9,53,54] The individual magnitude of the first is larger than that of the second, and an overall endothermic effect dominates. Solvent disruption in the microenvironment of dispersed droplets compensates for their organization during the clustering and hence accounts for positive ΔS_{cl}^{o}.

A comparison of ΔH_{cl}^{o} and ΔS_{cl}^{o} values in the absence and presence of Ph_2Se_2 reveals that both parameters decrease in magnitude. The lowering of ΔS_{cl}^{o} indicates the restricted orientation in the dispersion medium, whereas the low value of ΔH_{cl}^{o} depicts easily disturbable oil barriers surrounding the nanodroplets. From a thermodynamic point of view, it can be interpreted that the microemulsion without any additive represents a more organized system.

Spectral Analysis. The hydration of surfactant with solubilized water in reverse micelles and microemulsions has been the subject of investigation for decades. The results obtained by NMR and FT-IR as well as physicochemical studies showed that both the cation and anion of the surfactant are hydrated by the water molecules in the core of the aggregates.[55,56] Mcdonald et al.[57] revealed the existence of interfacial and bulk water, and Jain et al.[58] reported the presence of trapped, free, and bound water in the reverse micelles of AOT. Neuman and Park pointed out that solubilized water behaves differently from bulk water.[59] The FT-IR spectrum of the reverse micellar system is taken at different water contents in the region of 3000−3800 cm^{-1}. For the −OH stretching vibrations of the micellar system, the IR band appears in the region of 3050−3750 cm^{-1}. The band

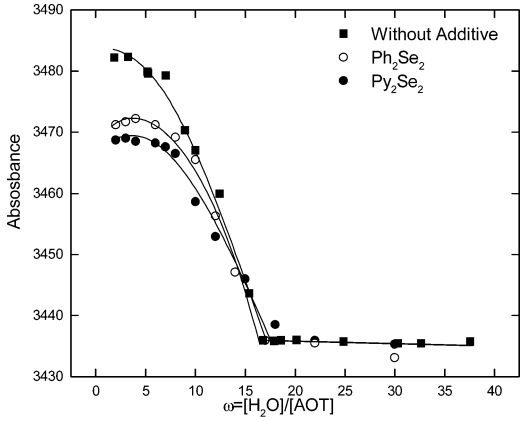

Figure 12. FT-IR absorbance of −OH functionality as a function of the water to surfactant molar ratio.

stretching depends on the water content of the system and any corresponding change occurring because of interactions with the additive.

The infrared spectrum of trapped water definitely differs from that of pure water, whose band precisely appears at 3400 cm^{-1}.[60] Figure 12 depicts the FT-IR stretching of −OH bond in the absence and in the presence of Py_2Se_2 and Ph_2Se_2 additives. We observe a decrease in the intensity of the −OH band with an increase in the ω value. The change in intensity becomes constant after a shoulder point (i.e., after $\omega = 16.85$). The effect of Py_2Se_2 and Ph_2Se_2 is visualized by a decrease in the frequency. A comparative analysis has been done for Py_2Se_2, Ph_2Se_2, and Ph_2Te_2 to analyze the solubilization process of water. A shift in the −OH stretching has been observed at constant composition for organochalcogen compounds as Ph_2Se_2 (3448.2 cm^{-1}) < Py_2Se_2 (3467.8 cm^{-1}) < Ph_2Te_2 (3544.1 cm^{-1}), as compared to 3400 cm^{-1} for pure water. The result indicates that the additive interacts with the core water. This confirms the inference drawn from conductivity results.

Conclusions

The effect of the dipyridyl and diphenyl derivatives of chalcogens (viz., Se and Te) has been investigated to locate the temperature percolation in the water/AOT/isooctane microemulsion. Conductivity−temperature plots show a sharp increase in the conductance after a threshold value corresponding to θ_c. Percolation has been explained on the basis of the easier channel formation and the resultant hopping of the surfactant counterion (Na^+) pertaining to percolation-assisting or -resisting additives. Py and Py_2Se_2 (only 5 mM) are seen to favor the onset of percolation. The phenyl derivative absolutely hinders the droplet association. A comparison of the additive (= 30 mM) efficiency in altering θ_c is Py < without additive < Py_2Se_2 ≤ Ph_2Se_2 < Ph_2Te_2. An increase in the droplet size decreases θ_c at low ω and equalizes θ_c at high ω. Droplets associated with the organochalcogens require high activation energy for the transport of Na^+. An intriguing correlation of ΔE_p with θ_c has been obtained. The ΔG_{cl}^{o} values have been estimated using the association model and are negative for the studied systems. During the clustering and redispersal of droplets, an endothermic process accompanied by positive entropy has been observed. In the presence of additives, the values of ΔH_{cl}^{o} and ΔS_{cl}^{o} are considerably low, indicating the easily disturbable surroundings. FT-IR spectroscopy revealed that core water mimics bulk water. The presence of the phenyl derivative in the system does not significantly alter the nature of trapped water.

Acknowledgment. This paper is dedicated to the fond memories of Prof. R.C. Paul (1919−2002). We are thankful to DST, New Delhi for financial assistance via grant nos. DST SP/SI/H51/98 (to SKM) and DST SR/SI/K-02/2003 (to KKB).

References and Notes

(1) Schelly, Z. A. *Curr. Opin. Colloid Interface Sci*. **1997**, *2*, 34.
(2) Solans, C.; Garcio-Celma, M. J. *Curr. Opin. Colloid Interface Sci*. **1997**, *2*, 464.
(3) Nagarajan, R.; Ruckenstein, E. *Langmuir* **2000**, *16*, 6400.
(4) Avramiotis, S.; Stamatis, H.; Kolisis, F. N.; Lianos, P.; Xenakis, A. *Langmuir* **1996**, *12*, 6320.
(5) Li, Q.; Li, T.; Wu, J. *Colloids Surf.* **2002**, *197*, 101.
(6) Dutta, P.; Sen, P.; Mukherjee, S.; Halder, A.; Bhattacharyya, K. *J. Phys. Chem. B* **2003**, *107*, 10815.
(7) Kuno, M.; Higginson, K. A.; Qadri, S. B.; Yousuf, M.; Lee, S. H.; Davis, B.; Mattoussi, H. *J. Phys. Chem. B* **2003**, *107*, 5758.
(8) Hait, S. K.; Sanyal, A.; Moulik, S. P. *J. Phys. Chem. B* **2002**, *106*, 12642.
(9) Hait, S. K.; Moulik, S. P.; Rodgers, M. P.; Bruke, S. E.; Palepu, R. *J. Phys. Chem. B* **2001**, *105*, 7145.
(10) Moulik, S. P.; De, G. C.; Bhowmik, B. B.; Panda, A. K. *J. Phys. Chem. B* **1999**, *103*, 7122.
(11) Mathew, C.; Patanjali, P. K.; Nabi, A.; Maitra, A. *Colloids Surf.* **1988**, *30*, 253.
(12) Ajith, S.; Rakshit, A. K. *Langmuir* **1995**, *11*, 1122.
(13) Garcia-Rio, L.; Leis, J. R.; Mejuto, J. C.; Pena, M. E.; Iglesias, E. *Langmuir* **1994**, *10*, 1676.
(14) Sen, S.; Dutta, P.; Sukul, D.; Bhattacharyya, K. *J. Phys. Chem. A* **2002**, *106*, 6017.
(15) (a) Alvarez, E.; Garcia-Rio, L.; Leis, J. R.; Mejuto, J. C.; Navaza, J. M. *J. Chem. Eng. Data* **1998**, *43*, 123. (b) Alvarez, E.; Garcia-Rio, L.; Mejuto, J. C.; Navaza, J. M. *J. Chem. Eng. Data* **1998**, *43*, 433. (c) Alvarez, E.; Garcia-Rio, L.; Mejuto, J. C.; Navaza, J. M. *J. Chem. Eng. Data* **1998**, *43*, 519. (d) Alvarez, E.; Garcia-Rio, L.; Mejuto, J. C.; Navaza, J. M. *J. Chem. Eng. Data* **1999**, *44*, 484.
(16) (a) Meier, W. *Langmuir* **1996**, *12*, 1188. (b) Meier, W. *Langmuir* **1996**, *12*, 6341.
(17) Mukhopadhyay, L.; Bhattacharya, P. K.; Moulik, S. P. *Colloids Surf.* **1990**, *50*, 295.
(18) Dasilva-Carvalhal, J.; Garcia-Rio, L.; Gomez-Diaz, D.; Mejuto, J. C.; Rodriguez-Dafonte, P. *Langmuir* **2003**, *19*, 5975.
(19) Dogra, A.; Rakshit, A. K. *J. Phys. Chem. B* **2004**, *108*, 10053.
(20) Hamilton, R. T.; Billman, J. F.; Kaler, E. W. Moha, Q.; Peyrelasse, J.; Boned, C. *Phys. Rev. A* **1987**, *35*, 3027.
(21) Meier, W.; Eicke, H.-F. *Curr. Opin. Colloid Interface Sci*. **1996**, *1*, 279.
(22) Mehta, S. K.; Kawaljit *Phys. Rev. E* **2002**, *65*, 021502.
(23) Giri, M. G.; Carla, M.; Gambi, C. M. C.; Senatra, D.; Chittofrati, A.; Sanguineti, A. *Phys Rev. A* **1994**, *50*, 1313.
(24) (a) Feldman, Y.; Kozlovich, N.; Nir, I.; Garti, N. *Phys. Rev. E* **1995**, *51*, 478. (b) Feldman, Y.; Kozlovich, N.; Nir, I.; Garti, N.; Archipov, V.; Idiyatullin, Z.; Zuev, Y.; Fedotov, V. *J. Phys. Chem*. **1996**, *100*, 3745.
(25) Haller, W. S.; Irgolic, K. J. *J. Organomet. Chem.* **1972**, *38*, 97.
(26) Reich, H. J.; Renga, J.-M.; Reich, I. L. *J. Am. Chem. Soc.* **1975**, *97*, 5434.
(27) Bhasin, K. K.; Jain, V. K.; Kumar, H.; Sharma, S.; Mehta, S. K.; Singh, J. *Synth. Commun.* **2003**, *33*, 977.
(28) Eicke, H. F.; Borkovec, M.; Gupta, B. D. *J. Phys. Chem*. **1989**, *93*, 314.
(29) Hait, S. K.; Moulik, S. P.; Palepu, R. *Langmuir* **2002**, *18*, 2471.
(30) Maitra, A.; Mathew, C.; Varshney, M. *J. Phys. Chem.* **1990**, *94*, 5290.
(31) *The Chemistry of Organic Selenium and Tellurium Compounds*; Patai, S., Rappoport, Z., Eds.; Wiley: New York, 1986; p 1.
(32) Alexandridis, P.; Holzwarth, J. F.; Hatton, T. A. *J. Phys. Chem*. **1995**, *99*, 8222.
(33) Zulauf, M.; Eicke, H.-F. *J. Phys. Chem*. **1979**, *83*, 480.
(34) Hou, M.-J.; Kim, M.; Shah, D. O. *J. Colloid Interface Sci.* **1988**, *123*, 398.
(35) Cametti, C.; Bordi, F. *Colloid Polym. Sci*. **1998**, *276*, 1044.
(36) Hou, M.-J.; Shah, D. O. *Langmuir* **1987**, *3*, 1086.
(37) Lagues, M. J. *Phys. (France) Lett*. **1978**, *39*, L487.
(38) Antalek, B.; Williams, A. J.; Texter, J.; Feldman, Y.; Garti, N. *Colloids Surf., A* **1997**, *128*, 1.
(39) Grannan, D. M.; Gailand, J. C.; Tanner, D. B. *Phys. Rev. Lett*. **1981**, *46*, 375.
(40) Sang, Y.; Noh, T. W.; Lee, S. I.; Gainis, J. R. *Phys. Rev. B* **1986**, *33*, 904.
(41) Lagues, M. *C. R. Acad Sci. URSS* **1978**, *25*, 278.
(42) Lagues, M.; Sauterey, C. *J. Phys. Chem*. **1980**, *84*, 1532.
(43) Mehta, S. K.; Bala, K. *Phys. Rev. E* **1995**, *51*, 5732.
(44) Grist, G. S.; Webman, I.; Safran, S. A.; Bug, A. L. R. *Phys. Rev. A* **1986**, *33*, 2842.
(45) Ponton, A.; Bose, T. K. *J. Chem. Phys.* **1991**, *94*, 6879.
(46) Kim, M. W.; Huang, J. S. *Phys. Rev. A* **1986**, *34*, 719.
(47) Bhattacharya, S.; Stokes, J. P.; Kim, M. W.; Huang, J. S. *Phys. Rev. Lett.* **1985**, *55*, 1884.
(48) Cametti, C.; Codastefano, P.; Tartaglia, P.; Chen, S.; Rouch, J. *Phys. Rev. A* **1992**, *45*, R5358.
(49) Mays, H.; Ilgenfritz, G. *J. Chem. Soc., Faraday Trans*. **1996**, *92*, 3145.
(50) Bordi, F.; Cametti, C.; Biasio, A. D. *Prog. Colloid Polym. Sci.* **1834**, *112*, 93.
(51) Napper, D. H. *Polymeric Stabilization of Colloidal Dispersions*; Academic: London, 1983.
(52) Piirma, I. *Polymeric Surfactants*; Surfactant Science Series; Marcel Dekker: New York, 1992; Vol. 42.
(53) Ray, S.; Bisal, S. R.; Moulik, S. P. *J. Chem. Soc., Faraday Trans*. **1993**, *89*, 3277.
(54) Moulik, S. P.; Ray, S. *Pure Appl. Chem*. **1994**, *66*, 521.
(55) Novaki, L. P.; Correa, N. M.; Silber, J. J.; El Seoud, O. A. *Langmuir* **2000**, *16*, 5573.
(56) Ide, M.; Yoshikawa, D.; Maeda, Y.; Kitano, H. *Langmuir* **1999**, *15*, 926.
(57) Macdonald, H.; Bedwell, B.; Guleri, E. *Langmuir* **1986**, *2*, 704.
(58) Jain, T. K.; Varshney, M.; Maitra, A. *J. Phys. Chem*. **1989**, *93*, 7409.
(59) Neumen, R. D.; Park, S. J. *J. Colloid Interface Sci.* **1992**, *152*, 41.
(60) Goffredi, M.; Liveri, V. T. *Prog. Colloid Polym. Sci*. **1999**, *112*, 109.